Mendelian randomization integrating GWAS and mQTL data identified novel pleiotropic DNA methylation loci for neuropathology of Alzheimer's disease

Di Liu[a], Youxin Wang[a], Huiquan Jing[a], Qun Meng[a,**], Jingyun Yang[b,c,d,e,*]

[a] Department of Epidemiology and Health Statistics, School of Public Health, Beijing Key Laboratory of Clinical Epidemiology, Capital Medical University, Beijing, China
[b] Division of Statistics, School of Economics, Shanghai University, Shanghai, China
[c] Research Center of Financial Information, Shanghai University, Shanghai, China
[d] Rush Alzheimer's Disease Center, Rush University Medical Center, Chicago, IL, USA
[e] Department of Neurological Sciences, Rush University Medical Center, Chicago, IL, USA

ARTICLE INFO

ABSTRACT

The pathogenesis of Alzheimer's disease (AD) remains largely unclear. Exploring the genetic/epigenetic loci showing pleiotropic association with the neuropathologies of AD may greatly enhance understanding of the mechanisms underlying the development of AD. In this study, using data from the Religious Orders Study and the Rush Memory and Aging Project, we undertook a Mendelian randomization approach integrating genome-wide association studies (GWASs) and DNA methylation quantitative trait locus data to explore pleiotropic epigenetic loci for AD neuropathologies, including amyloid-β (Aβ) load and tau-containing neurofibrillary tangle density. We performed GWASs of DNA methylation in brain tissues from 592 participants and mapped 60,595 cis-SNP-CpG pairs after correction for multiple testing. By linking cis-DNA methylation quantitative trait locus with GWAS results for Aβ load and tau tangles, we identified 47 CpGs showing pleiotropic association with Aβ load by the Mendelian randomization analysis. We then used gene expression data from 537 individuals and performed quantitative trait methylation analysis. We found that 18 of the 47 CpGs were in cis associated with 25 mRNAs/genes, comprising 41 unique CpG-mRNA/gene pairs. Our findings shed light on the role of DNA methylation in the pathogenesis of Aβ.

© 2020 Elsevier Inc. All rights reserved.

1. Introduction

Alzheimer's disease (AD), the most common neurodegenerative disease and a major cause of disability, affects patients' quality of life and brings a tremendous economic burden to the society (Alzheimer's Association, 2016; GBD, 2017 DALYs and HALE Collaborators, 2018). Neuropathologically, AD brains contain an extracellular buildup composed of amyloid-β (Aβ) peptide and intraneuronal accumulation of neurofibrillary tangles (NFTs) (Congdon and Sigurdsson, 2018; Ising and Heneka, 2018; Jansen et al., 2019; Kumar et al., 2020). However, the exact

neuropathogenesis of AD remains to be unclear. Therefore, it is important to further explore the pathological mechanisms underlying AD and identify genetic/epigenetic loci showing pleiotropic association with AD neuropathologies.

Although genome-wide association studies (GWASs) have revealed the complex genetic architecture of AD (Jansen et al., 2019; Lambert et al., 2013), the identified genetic variants only accounted for a portion of the heritability (Escott-Price et al., 2017; Sims et al., 2020). DNA methylation is an epigenetic marker that has been reported to play a key role in many biological processes and diseases (Ahuja et al., 2016; Horvath, 2012; Klose and Bird, 2006). Previous methylome-wide association studies have been successful in identifying DNA methylation loci/regions associated with AD neuropathologies. For example, multiple differentially methylated probes in *ABCA7*, *B1N1*, and *SORL1*, differentially methylated regions, and variably methylated regions were found to be associated with the burden of AD neuropathologies or pathological diagnosis of AD (De Jager et al., 2014; Huo et al., 2019; Lunnon et al., 2014; Smith et al., 2018; Watson et al., 2016; Yu et al., 2015). However, these findings

could be subject to confounding factors and reverse causation that might influence the results. As a result, more studies are needed to explore pleiotropic DNA methylation loci for AD neuropathologies.

It is a major public health goal to identify modifiable causes of a disease/disorder to develop effective interventions or therapeutic strategies. However, risk factors identified by conventional observational epidemiology studies were often found to be misleading because the findings were subject to confounding, reverse causation, and selection bias (Lawlor et al., 2004; Lawlor and Smith, 2006). Randomized controlled trials (RCTs) are often considered to be the gold standard to make pleiotropic inferences as all the characteristics, except the exposure of interest, are comparable among the groups (Bhide et al., 2018). However, conduction of RCTs is time-consuming, expensive, and in some cases, the allocation of exposure is unethical or impractical.

Mendelian randomization (MR) refers to methods that use proxy of modifiable risk factors to examine the pleiotropic effect of these risk factors on diseases/disorders by using data from observational epidemiology studies without the need of conducting a conventional RCT (Emdin et al., 2017). MR uses instrumental variables (IVs) as the proxy to mimic randomization of individuals to an exposure to ensure comparability of individuals with respect to known/unknown confounding factors, thereby enabling the estimation of a pleiotropic association with an outcome (Lawlor et al., 2008). Genetic variants are often used as the IVs because random allocation of alleles of genetic variants occur during gamete formation, well before the exposure or outcome. Estimation of the pleiotropic association can be made because the inherited genetic variants are independent of potentially confounding factors.

Recently, a novel analytical framework was applied to evaluate the pleiotropic association between DNA methylation levels and diseases that could minimize confounding and reverse causation through an MR approach integrating cis-DNA methylation quantitative trait locus (cis-mQTL) and GWAS data (Hannon et al., 2017, 2018; Huan et al., 2019; Richardson et al., 2017, 2018). Here, we adopted this novel MR approach to search for DNA methylation loci showing pleiotropic association with AD neuropathologies and to explore functional mechanisms underlying the association of genetic variants with AD neuropathologies.

2. Materials and methods

2.1. Study participants

Data for the present study were drawn from the Religious Orders Study and the Rush Memory and Aging Project (ROSMAP), both of which are ongoing, prospective studies of brain aging and dementia in older individuals (Bennett et al., 2012b, 2018). All participants were free of dementia at enrollment and agreed to annual clinical evaluations and brain donation on death. The clinical evaluation includes detailed neurologic examination and clinical classification of dementia and AD (Bennett et al., 2018). Postmortem human dorsolateral prefrontal cortex (DLPFC) tissues were obtained from deceased participants to measure DNA methylation, gene expression, and neuropathological protein. More details regarding the design of the ROSMAP study can be found in previous publications (Bennett et al., 2012a,b, 2018).

Written informed consent was obtained from participants at the beginning of each study as was an Anatomical Gift Act. Participants also signed a repository consent to allow their data to be repurposed. Both studies were approved by the Institutional Review Board of the Rush University Medical Center. The ethics approval was given in compliance with the Declaration of Helsinki. The clinical data can be requested at https://www.radc.rush.edu/,and the omics data can be requested at https://www.synapse.org/.

2.2. Assessment of neuropathological phenotypes

All the data used in our analyses were collected by the ROSMAP study. The collection of whole blood and brain tissues was described previously (Bennett et al., 2018). Detailed procedures for postmortem brain examination and neuropathological phenotyping have been described previously (Yu et al., 2015). In brief, neuropathological hallmarks including Aβ and tau-containing NFTs were quantified across the brain in both studies. Aβ protein was identified by molecularly specific immunohistochemistry and quantified by imaging analysis, with values being summarized as percent area occupied by Aβ. Aβ scores in eight regions (i.e., the hippocampus, entorhinal cortex, midfrontal cortex, inferior temporal, angular gyrus, calcarine cortex, anterior cingulate cortex, and superior frontal cortex) were averaged. Tau protein was identified by molecularly specific immunohistochemistry (antibodies to abnormally phosphorylated tau protein, AT8). The cortical density (per mm^2) was determined using systematic sampling. Tau scores in the same eight regions were averaged. Both indices were square root transformed to approach a normal distribution. More information is available at https://www.radc.rush.edu.

2.3. Genotyping and genotype imputation

Genotyping was performed using the Affymetrix Genome-Wide Human SNP Array 6.0. Detailed information regarding the pipeline of quality control of the genotyping data was reported in previous publications (De Jager et al., 2012; Ng et al., 2017). Dosages for all single-nucleotide polymorphisms (SNPs) (>35 million) were imputed on the 1000 Genomes reference using BEAGLE 3.3.2. Imputed SNPs were filtered based on minor allele frequency > 0.01 and imputation info score > 0.3, yielding 7,321,515 imputed SNPs that were used for further cis-mQTL mapping.

2.4. DNA methylation profiling

DNA methylation data were generated using the 450K Illumina array from the DLPFC, and quality control was conducted as described previously (Ng et al., 2017). A total of 420,131 methylation sites (i.e., CpGs) remained after quality control, and all data had been adjusted for age at death, sex, and experimental batch (De Jager et al., 2014).

2.5. Gene expression data

Gene expression data were generated using RNA-seq from the DLPFC at an average sequence depth of 90 million reads. Detailed description of the data generation and processing was described previously (Ng et al., 2017). Only highly expressed genes were kept (mean expression > 2log2(FPKM)), resulting in 55,889 mRNA and 50,999 expressed genes.

2.6. Statistical and bioinformatics analysis

Using data collected from the ROSMAP study, we undertook an MR approach which included a series of analyses, to examine the pleiotropic association of DNA methylation with AD neuropathologies. We first performed a genome-wide mQTL analysis to identify SNPs associated with DNA methylation in participants with both genetic and DNA methylation data. The cis-mQTL analysis followed a similar approach to the one described in a previous study (Hannon et al., 2018). In brief, linear regression was performed to test the association between each SNP and CpG, with each individual CpG as the dependent variable and each individual SNP as the independent variable, adjusted for the first three principal components. In total,

7,321,515 imputed genetic variants against each of the 420,131 eligible CpGs were tested by using the R package "MatrixEQTL." SNPs within 1 Mb of a CpG site showing significant association with the CpG (known as cis-mQTLs) were identified. We applied a conservative multiple testing correction to define cis-mQTLs (i.e., 0.05/number of SNP-CpG pairs $= 1.35 \times 10^{-10}$) to reduce weak instrument bias in the MR analysis. In the case of multiple variants showing significant association with the same individual CpG, we chose the cis-mQTL variant with the smallest p-value as the IV for the CpG site. We then performed GWAS for AD neuropathologies, including Aβ load and tau-containing NFT density, adjusted for age at death, sex, education, and the first three principal components. MR was undertaken with DNA methylation as the exposure, AD neuropathology as the outcome, and cis-mQTL as the IV. The analysis was performed using the inverse variance–weighted method as implemented in the mr_ivw function of the R package "MendelianRandomization" (Yavorska and Burgess, 2017). In the context of a single genetic variant as the IV, this is equivalent to a Wald ratio approach that allows distinct or overlapping samples to be used for the genetic association analysis in MR (Teumer, 2018). The weight was set to be delta to include the second-order term from the delta expansion in the calculation of the standard error of the estimate. We used the observed correlation between DNA methylation and the corresponding AD neuropathology to account for the correlation between genetic association with DNA methylation and genetic association with AD neuropathologies because of the sample overlap (Yavorska and Burgess, 2017) (see the supplementary file for the R and shell codes used for the analyses). We used false discovery rate to adjust for multiple testing.

We performed the heterogeneity in dependent instruments (HEIDI) test, as provided in summary data−based MR (Zhu et al., 2016), to test the existence of linkage in the observed association. Rejection of the null hypothesis (i.e., $P_{HEIDI} < 0.05$) indicates that the observed association in MR might be due to two distinct genetic variants in high linkage disequilibrium with each other.

In addition, a cis-mRNA quantitative trait methylation analysis was performed to explore the association between the identified CpGs and gene expression in participants with both DNA methylation and gene expression data. A *cis*-CpG-mRNA pair was defined as the target CpG residing in ±10 kb of the corresponding gene encoding the mRNA (false discovery rate $p < 0.05$). In brief, linear regression was performed to test the association between each CpG and mRNA, with each individual mRNA as the dependent variable
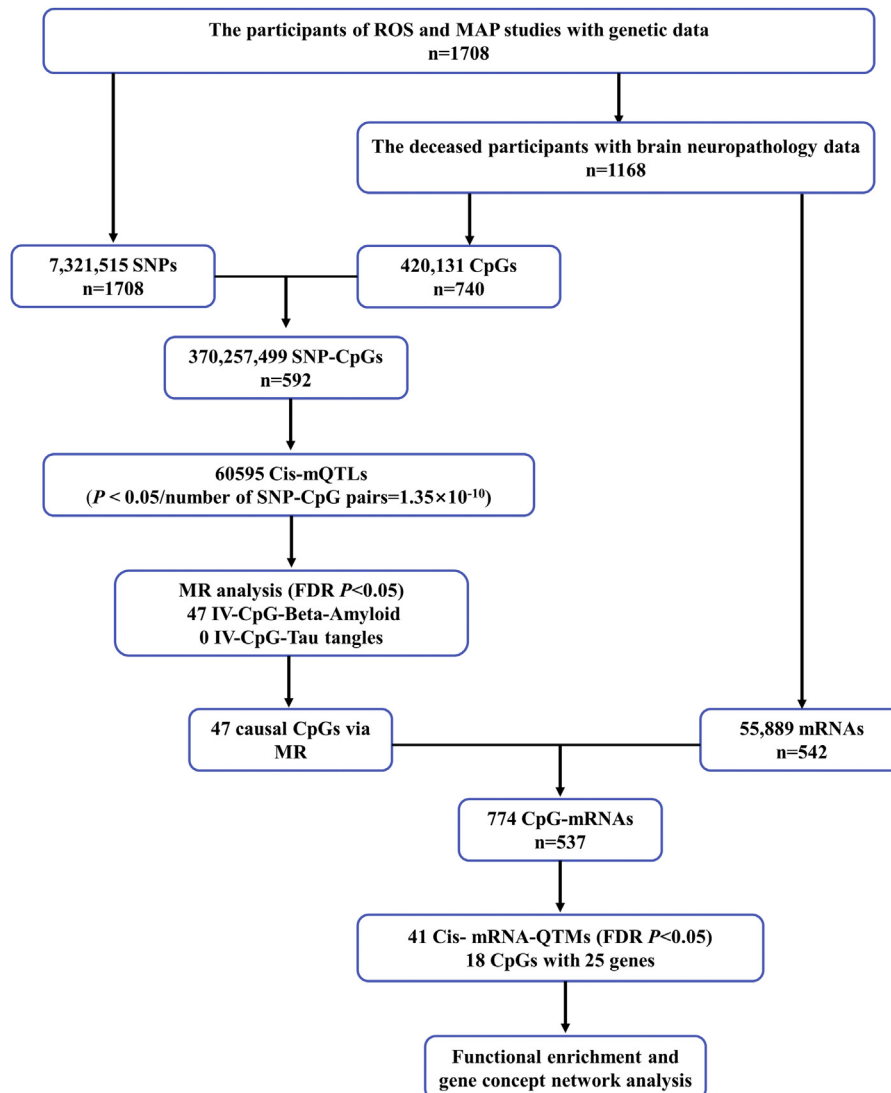

Fig. 1. The flow chart of bioinformatical/statistical analysis. Abbreviations: ROS, Religious Orders Study; MAP, Rush Memory and Aging Project; SNP, single-nucleotide polymorphism; mQTL, DNA methylation quantitative trait loci; FDR, false discovery rate; MR, Mendelian randomization.

and each individual CpG as the independent variable, adjusted for age at death, sex, education, and postmortem interval.

The annotations of transcripts were based on the Affymetrix exon array S1.0 platforms. To functionally annotate putative transcripts, we conducted functional enrichment analysis using the functional annotation tool "Metascape" (Zhou et al., 2019) and the gene concept network analysis using the R package "clusterProfiler" (Yu et al., 2012) for the genes harboring the identified CpGs and the cis-associated genes, separately. Gene symbols corresponding to putative genes ($p < 0.05$) were used as the input of the gene ontology (GO) and Kyoto Encyclopedia of Genes and Genomes enrichment analysis.

Data cleaning and statistical/bioinformatical analysis were performed using SAS, version 9.4 (SAS Institute, Inc., Cary, IL), R, version 4.0.0 (https://www.r-project.org/), PLINK 1.9 (https://www.cog-genomics.org/plink/1.9/), and summary data−based MR (https://cnsgenomics.com/software/smr/).

3. Results

3.1. The characteristics of the included participants

Fig. 1 is the flow chart showing the different stages of our analysis. Among the 1708 participants who had genetic data, 1312 died during follow-up (the mean age at death: 89.61 ± 6.42; male: 33.1%) and 1168 participants had brain neuropathology data, of whom 764 (65.4%) were diagnosed as having pathological AD. A total of 740 participants had methylation data, and 542 participants had gene expression data. Pairwise association analyses between genetic variants and DNA methylation were performed for 592 participants who had both genotype and methylation data (the mean age at death: 88.26 ± 6.47; male: 36.4%) for further cis-mQTL mapping and MR analysis. The cis paired association tests of the identified pleiotropic CpGs with mRNAs were performed in 537 participants (the mean age at death: 88.44 ± 6.70; male: 36.9%).

3.2. Putative pleiotropic CpGs for AD neuropathology

We identified more than 370 million cis-mQTL SNPs at $p < 0.05$ and found that 60,595 CpGs had at least one cis-mQTL SNP ($p < 1.35 \times 10^{-10}$; Fig. 2). We therefore selected the cis-mQTL variant with the smallest p-value as the IV for each CpG in the MR testing.

We undertook 60,595 tests to evaluate the pleiotropic associations between genetically determined DNA methylation and AD neuropathologies to explore putative pleiotropic effect of DNA methylation on AD neuropathology. MR analysis identified 47 pleiotropic associations between genetically determined CpGs and
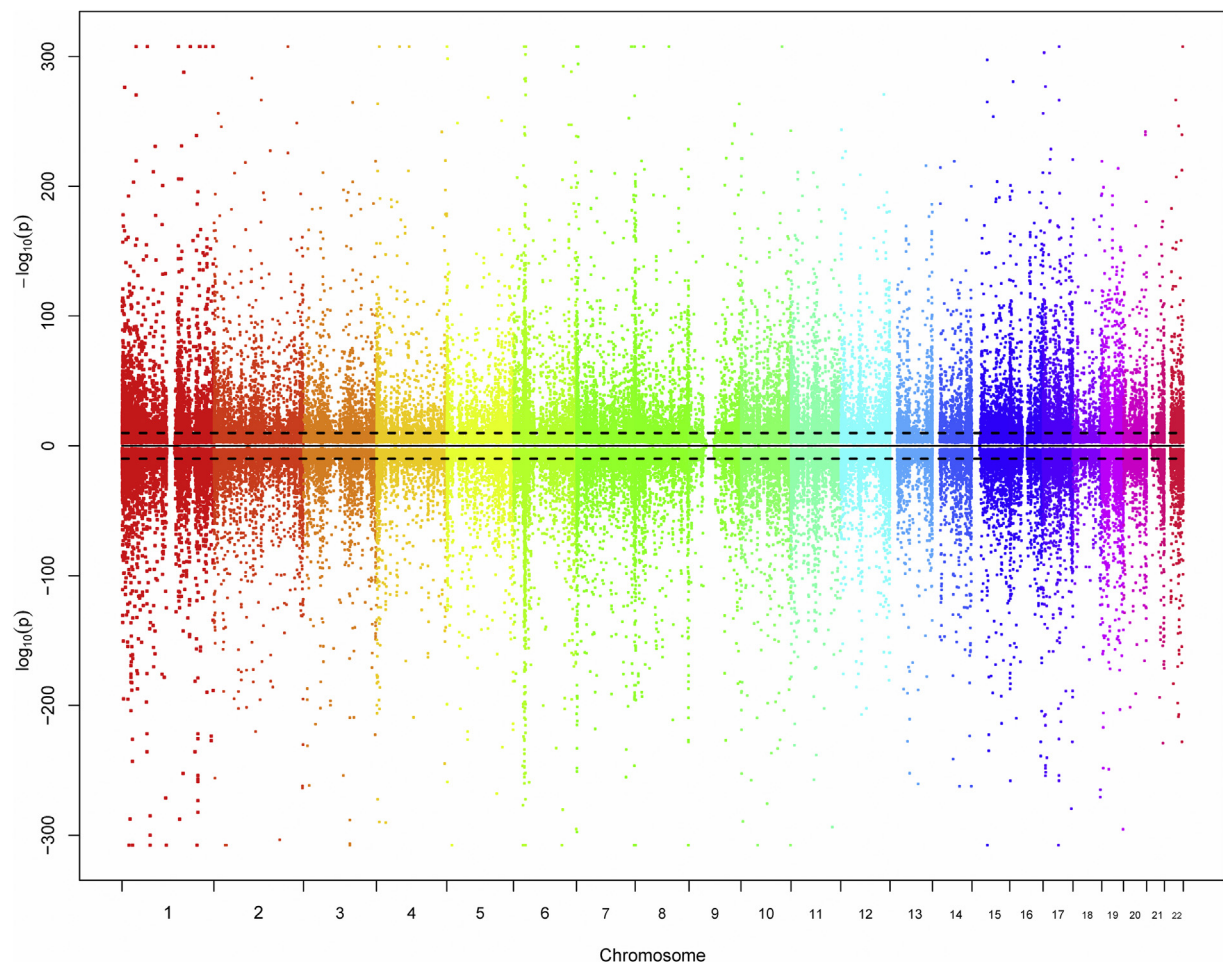
Fig. 2. Chicago plot for the association between cis-mQTLs and DNA methylation. We identified a total of 370,257,499 cis-mQTL SNPs at $p < 0.05$ using the R package "MatrixEQTL". In the plot, we only kept the cis-mQTL SNP having the smallest p-value for a CpG in the cases of multiple SNPs associated with the same CpG. Each point represents the association of a cis-mQTL SNP. The horizontal coordinate represents the location of a CpG within the chromosome, and the vertical coordinate is $-\log_{10}$ (p-value) if the association is positive and $\log_{10}$ (p-value) if the association is negative. The dashed line corresponds to the significance level using Bonferroni correction (1.35×10^{-10}). Abbreviations: mQTL, DNA methylation quantitative trait loci; SNP, single-nucleotide polymorphism.

Table 1
The characteristics of cis-mQTLs

CHR	SNP	CpG	Gene	Beta	SE	*p*-value
2	rs2373298	cg04480325	Intergenic	−0.039	0.005	1.92×10^{-16}
2	rs2373298	cg04521224	Intergenic	−0.026	0.003	5.18×10^{-15}
2	chr2:37987728	cg06480171	Intergenic	−0.017	0.002	9.71×10^{-13}
2	rs2373298	cg24523650	*EIF2AK2*	−0.079	0.006	2.64×10^{-34}
3	rs3009045	cg04863667	Intergenic	−0.036	0.004	6.81×10^{-15}
10	rs1751949	cg00730780	*KIAA1462*	−0.019	0.003	7.29×10^{-11}
10	rs2768668	cg01062834	*KIAA1462*	−0.009	0.001	4.58×10^{-12}
10	rs2768668	cg03325931	*BAMBI*	−0.018	0.003	5.57×10^{-12}
10	rs2768668	cg08461107	*KIAA1462*	0.021	0.003	1.25×10^{-14}
10	rs2768668	cg11614536	*KIAA1462*	−0.014	0.001	5.52×10^{-21}
10	rs71492582	cg11902278	*SVIL*	−0.034	0.003	1.19×10^{-28}
10	rs2768668	cg16513467	*WAC*	−0.007	0.001	6.98×10^{-15}
10	rs2768668	cg17428896	*SVIL*	−0.031	0.004	2.86×10^{-15}
10	rs71492582	cg18975376	*BAMBI*	−0.017	0.002	6.03×10^{-19}
10	rs1751947	cg19359767	Intergenic	−0.024	0.003	6.68×10^{-13}
10	rs71492582	cg19826211	*KIAA1462*	−0.01	0.001	1.17×10^{-18}
10	rs71492581	cg20628376	Intergenic	−0.022	0.003	8.13×10^{-13}
10	rs71492581	cg27036936	*KIAA1462*	−0.023	0.003	5.01×10^{-15}
13	rs10161769	cg00473245	*RAB20*	−0.007	0.001	2.15×10^{-14}
13	rs10161769	cg02742906	Intergenic	0.019	0.002	2.53×10^{-18}
13	rs10161769	cg08152546	Intergenic	0.013	0.002	2.72×10^{-15}
13	rs10161769	cg09469566	Intergenic	0.018	0.002	1.29×10^{-14}
13	rs10161769	cg10372485	*CARS2*	0.009	0.001	1.61×10^{-12}
13	rs10161769	cg15182896	Intergenic	0.025	0.002	1.53×10^{-24}
13	rs10161769	cg15270851	*CARS2*	0.008	0.001	1.89×10^{-16}
13	rs10161769	cg17488929	Intergenic	0.016	0.002	2.07×10^{-17}
13	rs10161769	cg17633592	Intergenic	0.011	0.001	2.39×10^{-13}
13	rs10161769	cg18541254	Intergenic	0.011	0.002	7.95×10^{-11}
13	rs10161769	cg18973457	Intergenic	0.004	0.001	2.81×10^{-11}
13	rs10161769	cg19246801	Intergenic	0.014	0.002	5.40×10^{-11}
13	rs10161769	cg20829347	*SOX1*	0.006	0.001	1.72×10^{-12}
13	rs10161769	cg21054521	Intergenic	0.02	0.003	5.71×10^{-12}
13	rs10161769	cg23119039	*COL4A2*	0.029	0.003	7.25×10^{-17}
13	rs10161769	cg23934404	Intergenic	0.012	0.002	2.89×10^{-13}
13	rs10161769	cg24074965	Intergenic	0.013	0.002	1.49×10^{-14}
13	rs10161769	cg25554685	Intergenic	0.012	0.001	5.13×10^{-16}
17	rs2159085	cg03363653	*C17orf76*	−0.017	0.002	4.31×10^{-18}
17	rs2159085	cg05090851	*UBB*	−0.006	0.001	6.08×10^{-11}
17	rs2159085	cg09105334	Intergenic	−0.082	0.006	8.74×10^{-37}
17	rs2159085	cg13180678	*CENPV*	−0.016	0.002	3.42×10^{-12}
17	rs2159085	cg18002814	*FAM18B2*	−0.014	0.002	2.31×10^{-11}
17	rs2159085	cg20577663	*CDRT4*	−0.027	0.003	2.58×10^{-21}
17	rs2159085	cg22229594	*PMP22*	−0.006	0.001	6.92×10^{-11}
17	rs2159085	cg24443925	*NCOR1*	0.012	0.001	3.08×10^{-20}
17	rs2159085	cg26744387	*C17orf76*	−0.013	0.002	3.26×10^{-14}
17	rs2159085	cg27131197	Intergenic	−0.043	0.005	2.05×10^{-17}
18	rs56945077	cg03671802	*RAX*	0.043	0.004	1.58×10^{-22}

Analyses were performed using the R package "MatrixEQTL", and multiple testing was used (i.e., 0.05/number of SNP-CpG pairs = 1.35×10^{-10}).
Beta is the estimated effect size.
Key: CHR, chromosome; SNP, single-nucleotide polymorphism; mQTL, quantitative trait loci; SE, standard error of the effect size.

Aβ load, including 44 positive associations and 3 negative associations with Aβ load, but no significant pleiotropic association between genetically determined CpGs and tau tangles (Table 1, Supplementary Table 1 and Fig. 3).

Of the 47 identified CpGs, 26 were located in the intragenic region, with approximately 70% located in the gene body (including 5′untranslated region, coding sequence, intron, and 3′untranslated region) and 30% in the transcription start site, and the remaining 21 in intergenic regions (Supplementary Table 2). Examination by chromatin states revealed that most of the identified CpGs were in strong transcription and promoter sites. More information of the pleiotropic CpGs can be found in Supplementary Table 2.

3.3. Association of the pleiotropic CpGs with mRNAs

To further dissect the relationship between DNA methylation and Aβ load, we evaluated the influence of the methylation levels on gene expression. We identified 774 CpG-mRNA pairs using cis-mRNA quantitative trait methylation analysis. Among the 47

CpGs, 18 CpGs were in cis associated with 25 mRNAs involved in 25 genes comprising 41 CpG-mRNA/gene pairs (Table 2). We found that 24 CpGs were positively associated with mRNAs and 17 CpGs negatively associated with mRNAs.

3.4. Pathway analysis/functional informatics

GO enrichment analysis of biological process, molecular function, and cellular component pathways showed that the genes harboring the identified CpGs were involved in four GO terms, including the nervous system development (R-HSA-9675108), forebrain development (GO:0030900), signaling by TGF-beta receptor complex (R-HSA-170834), and stress-activated MAPK cascade (GO:0051403; Fig. 4A). Concept network analysis of genes harboring the identified CpGs revealed multiple domains related with neuron generation, development, and differentiation (Fig. 4B). GO enrichment analysis of cis-associated genes identified only one significant GO term of the Golgi vesicle transport (GO:0048193; Fig. 4C). Concept network analysis of cis-associated genes revealed
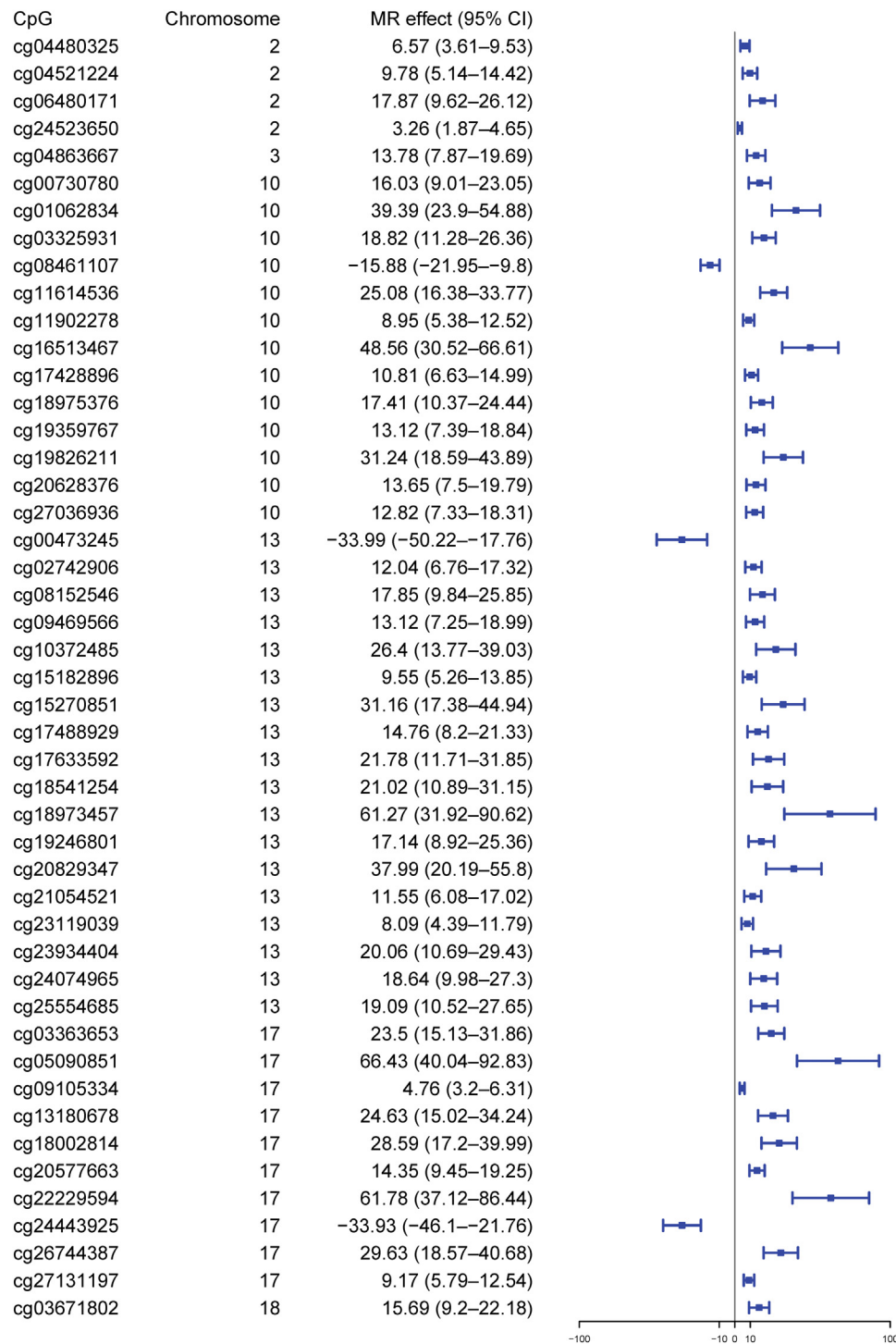
CpG	Chromosome	MR effect (95% CI)
cg04480325	2	6.57 (3.61–9.53)
cg04521224	2	9.78 (5.14–14.42)
cg06480171	2	17.87 (9.62–26.12)
cg24523650	2	3.26 (1.87–4.65)
cg04863667	3	13.78 (7.87–19.69)
cg00730780	10	16.03 (9.01–23.05)
cg01062834	10	39.39 (23.9–54.88)
cg03325931	10	18.82 (11.28–26.36)
cg08461107	10	−15.88 (−21.95–−9.8)
cg11614536	10	25.08 (16.38–33.77)
cg11902278	10	8.95 (5.38–12.52)
cg16513467	10	48.56 (30.52–66.61)
cg17428896	10	10.81 (6.63–14.99)
cg18975376	10	17.41 (10.37–24.44)
cg19359767	10	13.12 (7.39–18.84)
cg19826211	10	31.24 (18.59–43.89)
cg20628376	10	13.65 (7.5–19.79)
cg27036936	10	12.82 (7.33–18.31)
cg00473245	13	−33.99 (−50.22–−17.76)
cg02742906	13	12.04 (6.76–17.32)
cg08152546	13	17.85 (9.84–25.85)
cg09469566	13	13.12 (7.25–18.99)
cg10372485	13	26.4 (13.77–39.03)
cg15182896	13	9.55 (5.26–13.85)
cg15270851	13	31.16 (17.38–44.94)
cg17488929	13	14.76 (8.2–21.33)
cg17633592	13	21.78 (11.71–31.85)
cg18541254	13	21.02 (10.89–31.15)
cg18973457	13	61.27 (31.92–90.62)
cg19246801	13	17.14 (8.92–25.36)
cg20829347	13	37.99 (20.19–55.8)
cg21054521	13	11.55 (6.08–17.02)
cg23119039	13	8.09 (4.39–11.79)
cg23934404	13	20.06 (10.69–29.43)
cg24074965	13	18.64 (9.98–27.3)
cg25554685	13	19.09 (10.52–27.65)
cg03363653	17	23.5 (15.13–31.86)
cg05090851	17	66.43 (40.04–92.83)
cg09105334	17	4.76 (3.2–6.31)
cg13180678	17	24.63 (15.02–34.24)
cg18002814	17	28.59 (17.2–39.99)
cg20577663	17	14.35 (9.45–19.25)
cg22229594	17	61.78 (37.12–86.44)
cg24443925	17	−33.93 (−46.1–−21.76)
cg26744387	17	29.63 (18.57–40.68)
cg27131197	17	9.17 (5.79–12.54)
cg03671802	18	15.69 (9.2–22.18)

Fig. 3. Forest plot for the estimated MR effects and 95% confidence intervals for the casual associations of CpGs with Aβ load. Analyses were performed using the R package "'MendelianRandomization", and multiple testing was adjusted using the false discovery rate. Abbreviations: Aβ, amyloid beta; MR, Mendelian randomization; CI, confidence interval.

domains associated with leukocyte deregulation and DNA damage recognition (Fig. 4D). More information can be found in Fig. 4 and Supplementary Tables 3–4

4. Discussion

In this study, we integrated the GWAS and mQTL data in MR analysis to explore putative pleiotropic DNA methylation loci for AD neuropathology. We identified 47 pleiotropic DNA methylation loci for Aβ load. Among the 47 CpGs, 18 CpGs were associated in cis with 25 mRNAs involved in 25 genes comprising 41 CpG-mRNA/gene pairs. To the best of our knowledge, this is the first study to examine putative pleiotropic epigenetic loci for AD neuropathology through an MR approach.

Evidence is accumulating that DNA methylation is related to AD (De Jager et al., 2014; Huo et al., 2019; Lunnon et al., 2014; Smith et al., 2018; Yu et al., 2015). However, previous studies focusing on exploring the association between differential DNA methylation

Table 2
The characteristics of cis-mRNA-QTMs

CHR	CpG	Gene_ID	Gene	Beta	SE	*p*-value	Q-value
17	cg20577663	ENSG00000170425.3	*ADORA2B*	17.54	3.14	3.85×10^{-8}	2.22×10^{-5}
17	cg20577663	ENSG00000109099.9	*PMP22*	96.78	18.44	2.22×10^{-7}	6.41×10^{-5}
10	cg18975376	ENSG00000095739.7	*BAMBI*	11.44	2.29	8.59×10^{-7}	1.65×10^{-4}
10	cg18975376	ENSG00000150051.8	*MKX*	−4.54	0.96	2.64×10^{-6}	3.79×10^{-4}
2	cg04521224	ENSG00000163171.6	*CDC42EP3*	−3.15	0.68	4.47×10^{-6}	5.15×10^{-4}
13	cg25554685	ENSG00000126218.7	*F10*	3.73	0.82	7.25×10^{-6}	6.96×10^{-4}
2	cg04521224	ENSG00000115825.5	*PRKD3*	3.17	0.71	1.14×10^{-5}	9.36×10^{-4}
17	cg20577663	ENSG00000175061.10	*C17orf76−AS1*	170.58	41.27	4.16×10^{-5}	3.00×10^{-3}
2	cg24523650	ENSG00000115825.5	*PRKD3*	1.52	0.38	7.33×10^{-5}	4.69×10^{-3}
17	cg27131197	ENSG00000141030.8	*COPS3*	−11.53	2.92	9.05×10^{-5}	4.94×10^{-3}
2	cg04480325	ENSG00000115825.5	*PRKD3*	1.98	0.5	9.44×10^{-5}	4.94×10^{-3}
10	cg18975376	ENSG00000150054.12	*MPP7*	−3.93	1.01	1.12×10^{-4}	5.37×10^{-3}
2	cg06480171	ENSG00000003509.11	*C2orf56*	−5.52	1.43	1.35×10^{-4}	5.97×10^{-3}
2	cg04480325	ENSG00000115828.11	*QPCT*	−5.88	1.59	2.42×10^{-4}	9.95×10^{-3}
13	cg24074965	ENSG00000139835.8	*GRTP1*	3.7	1.05	4.9×10^{-4}	0.019
13	cg24074965	ENSG00000185896.9	*LAMP1*	45.14	12.98	5.45×10^{-4}	0.019
17	cg20577663	ENSG00000170315.8	*UBB*	−917.99	264.05	5.5×10^{-4}	0.0198
2	cg06480171	ENSG00000163171.6	*CDC42EP3*	−3.89	1.12	5.82×10^{-4}	0.019
10	cg03325931	ENSG00000150051.8	*MKX*	−2.23	0.65	6.8×10^{-4}	0.02
10	cg01062834	ENSG00000183621.10	*ZNF438*	6.28	1.86	7.86×10^{-4}	0.021
10	cg19826211	ENSG00000183621.10	*ZNF438*	8.1	2.4	7.91×10^{-4}	0.021
2	cg04521224	ENSG00000115828.11	*QPCT*	−7.64	2.27	8.09×10^{-4}	0.021
17	cg27131197	ENSG00000170425.3	*ADORA2B*	5.68	1.69	8.54×10^{-4}	0.021
13	cg23119039	ENSG00000255874.1	*LINC00346*	0.27	0.08	8.79×10^{-4}	0.021
10	cg20628376	ENSG00000150051.8	*MKX*	−1.78	0.54	1.06×10^{-3}	0.022
13	cg25554685	ENSG00000057593.9	*F7*	−3.12	0.95	1.06×10^{-3}	0.022
17	cg13180678	ENSG00000197566.5	*ZNF624*	1.24	0.38	1.07×10^{-3}	0.022
2	cg04521224	ENSG00000003509.11	*C2orf56*	−2.87	0.88	1.12×10^{-3}	0.022
17	cg24443925	ENSG00000109099.9	*PMP22*	−130.38	39.93	1.16×10^{-3}	0.022
17	cg20577663	ENSG00000175106.12	*FAM18B2*	5.36	1.64	1.18×10^{-3}	0.022
17	cg18002814	ENSG00000170425.3	*ADORA2B*	15.83	4.85	1.18×10^{-3}	0.022
10	cg03325931	ENSG00000095739.7	*BAMBI*	5.01	1.57	1.50×10^{-3}	0.027
17	cg18002814	ENSG00000108474.8	*PIGL*	−10.7	3.37	1.57×10^{-3}	0.027
10	cg20628376	ENSG00000095787.15	*WAC*	20.19	6.36	1.59×10^{-3}	0.027
2	cg06480171	ENSG00000115825.5	*PRKD3*	3.74	1.18	1.65×10^{-3}	0.027
2	cg06480171	ENSG00000115828.11	*QPCT*	−11.64	3.73	1.89×10^{-3}	0.030
17	cg18002814	ENSG00000109099.9	*PMP22*	86.49	28.41	2.45×10^{-3}	0.038
13	cg24074965	ENSG00000057593.9	*F7*	−2.46	0.82	2.90×10^{-3}	0.044
13	cg10372485	ENSG00000088448.9	*ANKRD10*	27.55	9.26	3.06×10^{-3}	0.045
2	cg24523650	ENSG00000115808.7	*STRN*	0.65	0.22	3.15×10^{-3}	0.045
17	cg13180678	ENSG00000214941.3	*ZSWIM7*	27.71	9.42	3.41×10^{-3}	0.048

Results were obtained using linear regression, adjusting for age at death, sex, and education, and multiple testing were adjusted using the false discovery rate (Q value < 0.05). Beta is the estimated effect size.
Key: CHR, chromosome; QTM, quantitative trait methylation; SE, standard error.

and AD are prone to confounding and reverse causation (Dekkers et al., 2016; Huo et al., 2019; Wahl et al., 2017). As a result, some disease-associated CpGs from methylome-wide association studies may reflect the influence of the diseases on DNA methylation rather than the pleiotropic effects of DNA methylation on the diseases. By contrast, MR incorporates cis-mQTL information into GWAS analyses and has the potential to increase the power of GWAS in identifying pleiotropic loci associated with complex diseases (Hannon et al., 2017, 2018; Richardson et al., 2017). This novel analytical framework that integrates GWAS and mQTL data in MR analysis enabled us to identify multiple epigenetic loci that showed a pleiotropic relationship with Aβ load, indicating that DNA methylation resides along the pleiotropic pathway linking genetic variants with AD neuropathology.

Some of the pleiotropic CpGs identified in our study have been reported to be associated with Aβ load or AD-related risk factors. For example, the epigenetic locus cg24523650 in *EIF2AK2* was associated with Aβ load by a previous epigenome-wide association study of AD neuropathology (Huo et al., 2019). Two other methylation loci, cg08152546 and cg13180678, which reside in or are close to *CENPV*, were associated with aging (Florath et al., 2014; Weidner et al., 2014), a major risk factor for AD. In addition, we identified several pleiotropic epigenetic loci, such as cg00473245 in *RAB20*

and cg27036936 in *KIAA1462*, that were associated with metabolism-related disorders such as metabolic syndrome, obesity, and diabetes (Akinyemiju et al., 2018; Nilsson et al., 2014). Increasing evidence suggests epidemiological and pathological links between AD and metabolic traits (Jansen et al., 2019; Sims et al., 2020). Previous research identified common genetic architectures shared between AD and metabolic traits and shed light on molecular mechanisms underlying the association between AD and metabolic dysregulation (Zhu et al., 2019). Whether and how these identified epigenetic loci affect the risk of AD via metabolic pathways warrants further investigation.

Some of the genes harboring the identified CpGs were reported to be involved in the development of the nervous system or AD neuropathologies. For example, we identified cg20829347 in *SOX1* as a pleiotropic epigenetic site for Aβ load. *SOX1* encodes a member of the SOX (SRY-related high mobility group box) family of transcription factors and was reported to be involved in the regulation of embryonic development and in the determination of cell fate (Berger et al., 2016). *SOX1* plays an important role in regulating neurogenesis in the nervous system (Kan et al., 2004). In addition, we found cg05090851 in *UBB* as a pleiotropic epigenetic site for Aβ load. *UBB* encodes ubiquitin, which has a major role in targeting cellular proteins for degradation and is also involved in the
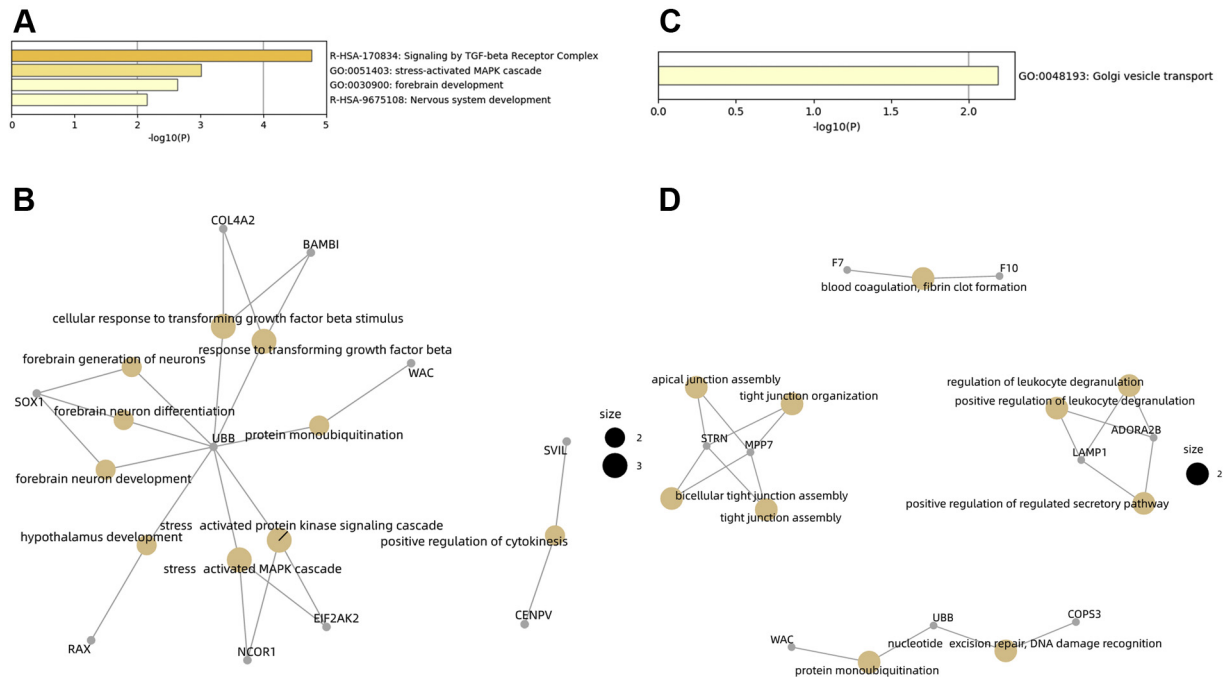
Fig. 4. Functional enrichment and gene concept network analysis. (A) Enriched GO terms based on genes harboring the identified CpGs; (B) concept network analysis of the genes harboring the identified CpGs; (C) enriched GO terms based on cis-associated genes; and (D) concept network analysis of the cis-associated genes. Abbreviation: GO, gene ontology.

maintenance of chromatin structure, regulation of gene expression, and stress response (Grumati and Dikic, 2018). An aberrant form of ubiquitin was found to be accumulated in brain tissues of patients with AD (Munari et al., 2018).

Although it is widely hypothesized that DNA methylation could influence gene expression, its relationship with transcriptional activity in influencing AD neuropathology is not fully understood. We found that two of the identified CpGs (cg18975376 and cg03325931) were associated with the expression of *BAMBI*, which encodes a transmembrane glycoprotein related to transforming growth factor beta type I (TGF-β1) family (Bai et al., 2017). It was found that impairment of TGF-β1 signaling was associated with exacerbated Aβ deposition and NFT formation (Estrada et al., 2018). In addition, many of the identified pleiotropic CpGs for Aβ load showed in cis association with genes might be involved in AD neuropathologies. For example, cg04480325, cg04521224, and cg06480171, located in the intergenic region, were associated in cis with the expression of *QPCT* that encodes human pituitary glutaminyl cyclase and is responsible for the presence of pyroglutamyl residues in many neuroendocrine peptides. It was found that lowering QPCT expression could reduce the amount of pyroglutamate-Aβ, a major constituent of Aβ deposits in human AD (Alexandru et al., 2011).

We also found that some of identified pleiotropic CpGs were in cis associated with genes that have not been reported to be involved in the pathogenesis of AD. For example, cg20577663 in *CDRT4* was in cis associated with the expression of *ADORA2B* that encodes an adenosine receptor. Adenosine receptor signaling plays important roles in normal physiology and was reported to be involved in cardiovascular diseases (Geldenhuys et al., 2017; Gile and Eckle, 2016; Novotný, 2015). In addition, cg24523650 in *EIF2AK2* was in cis associated with the expression of *STRN* that encodes striatin, a cell-cell junctional protein involved in maintaining correct cell adhesion (Lahav-Ariel et al., 2019). More studies are needed to reveal the exact function of these genes in the development of AD neuropathology.

Our study has some strengths. The ROSMAP have similar procedures in the collection of 'omics' data and pathologic data, which allows various types of data to be merged for analyses that may have small to moderate effects. The MR approach greatly reduced confounding bias and reverse causation. Therefore, the identified DNA methylation loci likely represent some 'true' pleiotropic epigenetic markers for AD neuropathology. The ROSMAP studies have a very high rate of participation in the follow-up and autopsy, which reduced bias from selective attrition. We only included study participants of European ancestry in our analyses and controlled for the first three principal components in the cis-mQTL analysis; therefore, population stratification is less likely to be a problem.

Our study also has some limitations. Our MR analysis was based on the following four assumptions: (1) the genotype is associated with DNA methylation; (2) the genotype is not associated with confounding factors that bias the associations between DNA methylation and Aβ load; (3) the genotype is related to Aβ load only via its association with DNA methylation; and (4) all the associations are linear and unaffected by statistical interaction. In the cis-mQTL analysis, we filtered genetic variants with conservative multiple testing and chose the genetic variant with the smallest *p*-value for each CpG, minimizing the concern of weak IV (assumption 1). Nonassociation of the genotype with confounders is often based on the biological belief that the genotype will not be associated with socioeconomic and behavioral characteristics that commonly confound the effects of exposure (i.e., DNA methylation) on the outcome (i.e., Aβ load) (Lawlor et al., 2008). Moreover, we used data from the same studies in obtaining both genotype-DNA methylation and genotype-Aβ load estimates, further alleviating the concern about violation of assumption 2 (Lawlor et al., 2008). Regarding assumption 3, we acknowledge that with the use of single variant–based MR method, we could not rule out the possibility of horizontal pleiotropy which could distort the MR results. A recent study found that horizontal pleiotropy was detectable in approximately 50% of significant causal relationships in MR and could induce severe distortions in MR estimates as well as around

10% of false-positive causal relationships (Verbanck et al., 2018). We performed the HEIDI test and found that of the 47 identified CpGs, the test was available for 16 CpGs. The HEIDI test was not significant for most CpGs except one (cg03671802 in *RAX*; Supplementary Table 1), indicating that these observed associations were less likely subject to horizontal pleiotropy. However, caution should still be executed in interpreting the MR results because the HEIDI test was not feasible for the remaining identified CpGs. It is often difficult to validate the linearity assumption (Lawlor et al., 2008). Violation of the assumption is not essential when the purpose is to test the null hypothesis of no effect of the exposure (e.g., DNA methylation) on the outcome (e.g., Aβ load), but can cause problems when the purpose is to estimate the size of the effect. We adopted correction for multiple testing to reduce the false positive rate; however, we may have missed important SNPs or methylation loci. Moreover, our pathway analysis only included pleiotropic methylation loci in association with gene expression, and we did not consider other methylation loci that could also affect the development of Aβ. More studies are needed to systematically explore the role of DNA methylation in influencing transcriptional activity in the neuropathogenesis of AD.

In conclusion, by performing multi-stage analyses incorporating GWAS and mQTL data through an MR approach, we identified multiple pleiotropic DNA methylation loci for Aβ load. Our findings shed light on the role of DNA methylation in the pathogenesis of Aβ load. Future studies are needed to validate our findings and elucidate the exact functions of the identified epigenetic loci and the associated genes in the development of AD neuropathology.

Disclosure statement

The authors have no conflict of interest to report.

CRediT authorship contribution statement

Di Liu: Formal analysis, Data curation, Writing - original draft, Writing - review & editing, Visualization. **Youxin Wang:** Conceptualization, Supervision. **Huiquan Jing:** Writing - review & editing. **Qun Meng:** Writing - review & editing. **Jingyun Yang:** Conceptualization, Methodology, Validation, Supervision.

Acknowledgements

The authors confirmed that all authors have reviewed the contents of the article being submitted, approved its contents, and validated the accuracy of the data.

Appendix A. Supplementary data

Supplementary data to this article can be found online at https://doi.org/10.1016/j.neurobiolaging.2020.09.019.

References

Ahuja, N., Sharma, A.R., Baylin, S.B., 2016. Epigenetic therapeutics: a new weapon in the war against cancer. Annu. Rev. Med. 67, 73.

Akinyemiju, T., Do, A.N., Patki, A., Aslibekyan, S., Zhi, D., Hidalgo, B., Tiwari, H.K., Absher, D., Geng, X., Arnett, D.K., Irvin, M.R., 2018. Epigenome-wide association study of metabolic syndrome in African-American adults. Clin. Epigenet 10, 49.

Alexandru, A., Jagla, W., Graubner, S., Becker, A., Bäuscher, C., Kohlmann, S., Sedlmeier, R., Raber, K.A., Cynis, H., Rönicke, R., Reymann, K.G., Petrasch-Parwez, E., Hartlage-Rübsamen, M., Waniek, A., Rossner, S., Schilling, S., Osmand, A.P., Demuth, H.U., von Hörsten, S., 2011. Selective hippocampal neurodegeneration in transgenic mice expressing small amounts of truncated Aâ is induced by pyroglutamate-Aâ formation. J. Neurosci. 31, 12790—12801.

Alzheimer's Association, 2016. 2016 Alzheimer's disease facts and figures. Alzheimers Dement. 12, 459—509.

Bai, L., Chu, G., Wang, W., Xiang, A., Yang, G., 2017. BAMBI promotes porcine granulosa cell steroidogenesis involving TGF-β signaling. Theriogenology 100, 24—31.

Bennett, D.A., Buchman, A.S., Boyle, P.A., Barnes, L.L., Wilson, R.S., Schneider, J.A., 2018. Religious orders study and rush memory and aging project. J. Alzheimers Dis. 64, S161—S189.

Bennett, D.A., Schneider, J.A., Arvanitakis, Z., Wilson, R.S., 2012a. Overview and findings from the religious orders study. Curr. Alzheimer Res. 9, 628—645.

Bennett, D.A., Schneider, J.A., Buchman, A.S., Barnes, L.L., Boyle, P.A., Wilson, R.S., 2012b. Overview and findings from the rush memory and aging project. Curr. Alzheimer Res. 9, 646—663.

Berger, B., Dersch, R., Ruthardt, E., Rasiah, C., Rauer, S., Stich, O., 2016. Prevalence of anti-SOX1 reactivity in various neurological disorders. J. Neurol. Sci. 369, 342—346.

Bhide, A., Shah, P.S., Acharya, G., 2018. A simplified guide to randomized controlled trials. Acta Obstet. Gynecol. Scand. 97, 380—387.

Congdon, E.E., Sigurdsson, E.M., 2018. Tau-targeting therapies for Alzheimer disease. Nat. Rev. Neurol. 14, 399—415.

De Jager, P.L., Shulman, J.M., Chibnik, L.B., Keenan, B.T., Raj, T., Wilson, R.S., Yu, L., Leurgans, S.E., Tran, D., Aubin, C., Anderson, C.D., Biffi, A., Corneveaux, J.J., Huentelman, M.J., Rosand, J., Daly, M.J., Myers, A.J., Reiman, E.M., Bennett, D.A., Evans, D.A., 2012. A genome-wide scan for common variants affecting the rate of age-related cognitive decline. Neurobiol. Aging 33, 1017.e1011-1015.

De Jager, P.L., Srivastava, G., Lunnon, K., Burgess, J., Schalkwyk, L.C., Yu, L., Eaton, M.L., Keenan, B.T., Ernst, J., McCabe, C., Tang, A., Raj, T., Replogle, J., Brodeur, W., Gabriel, S., Chai, H.S., Younkin, C., Younkin, S.G., Zou, F., Szyf, M., Epstein, C.B., Schneider, J.A., Bernstein, B.E., Meissner, A., Ertekin-Taner, N., Chibnik, L.B., Kellis, M., Mill, J., Bennett, D.A., 2014. Alzheimer's disease: early alterations in brain DNA methylation at ANK1, BIN1, RHBDF2 and other loci. Nat. Neurosci. 17, 1156—1163.

Dekkers, K.F., van Iterson, M., Slieker, R.C., Moed, M.H., Bonder, M.J., van Galen, M., Mei, H., Zhernakova, D.V., van den Berg, L.H., Deelen, J., van Dongen, J., van Heemst, D., Hofman, A., Hottenga, J.J., van der Kallen, C.J., Schalkwyk, C.G., Stehouwer, C.D., Tigchelaar, E.F., Uiterlinden, A.G., Willemsen, G., Zhernakova, A., Franke, L, T H.P.A., Jansen, R., van Meurs, J., Boomsma, D.I., van Duijn, C.M., van Greevenbroek, M.M., Veldink, J.H., Wijmenga, C., van Zwet, E.W., Slagboom, P.E., Jukema, J.W., Heijmans, B.T., 2016. Blood lipids influence DNA methylation in circulating cells. Genome Biol. 17, 138.

Emdin, C.A., Khera, A.V., Kathiresan, S., 2017. Mendelian randomization. JAMA 318, 1925—1926.

Escott-Price, V., Shoai, M., Pither, R., Williams, J., Hardy, J., 2017. Polygenic score prediction captures nearly all common genetic risk for Alzheimer's disease. Neurobiol. Aging 49, 214.e217-214.e211.

Estrada, L.D., Oliveira-Cruz, L, Cabrera, D., 2018. Transforming growth factor beta type I role in neurodegeneration: implications for Alzheimer's disease. Curr. Protein Pept. Sci. 19 (12), 1180—1188.

Florath, I., Butterbach, K., Muller, H., Bewerunge-Hudler, M., Brenner, H., 2014. Cross-sectional and longitudinal changes in DNA methylation with age: an epigenome-wide analysis revealing over 60 novel age-associated CpG sites. Hum. Mol. Genet. 23, 1186—1201.

GBD 2017 DALYs and HALE Collaborators, 2018. Global, regional, and national disability-adjusted life-years (DALYs) for 359 diseases and injuries and healthy life expectancy (HALE) for 195 countries and territories, 1990-2017: a systematic analysis for the Global Burden of Disease Study 2017. Lancet 392, 1859—1922.

Geldenhuys, W.J., Hanif, A., Yun, J., Nayeem, M.A., 2017. Exploring adenosine receptor ligands: potential role in the treatment of cardiovascular diseases. Molecules (Basel, Switzerland) 22.

Gile, J., Eckle, T., 2016. ADORA2b signaling in cardioprotection. J. Nat. Sci. 2.

Grumati, P., Dikic, I., 2018. Ubiquitin signaling and autophagy. J. Biol. Chem. 293, 5404—5413.

Hannon, E., Gorrie-Stone, T.J., Smart, M.C., Burrage, J., Hughes, A., Bao, Y., Kumari, M., Schalkwyk, L.C., Mill, J., 2018. Leveraging DNA-methylation quantitative-trait loci to characterize the relationship between methylomic variation, gene expression, and complex traits. Am. J. Hum. Genet. 103, 654—665.

Hannon, E., Weedon, M., Bray, N., O'Donovan, M., Mill, J., 2017. Pleiotropic effects of trait-associated genetic variation on DNA methylation: utility for refining GWAS loci. Am. J. Hum. Genet. 100, 954—959.

Horvath, S., 2012. Aging effects on DNA methylation modules in human brain and blood tissue. Genome Biol. 13, R97.

Huan, T., Joehanes, R., Song, C., Peng, F., Guo, Y., Mendelson, M., Yao, C., Liu, C., Ma, J., Richard, M., Agha, G., Guan, W., Almli, L.M., Conneely, K.N., Keefe, J., Hwang, S.J., Johnson, A.D., Fornage, M., Liang, L., Levy, D., 2019. Genome-wide identification of DNA methylation QTLs in whole blood highlights pathways for cardiovascular disease. Nat. Commun. 10, 4267.

Huo, Z., Zhu, Y., Yu, L., Yang, J., De Jager, P., Bennett, D.A., Zhao, J., 2019. DNA methylation variability in Alzheimer's disease. Neurobiol. Aging 76, 35—44.

Ising, C., Heneka, M.T., 2018. Functional and structural damage of neurons by innate immune mechanisms during neurodegeneration. Cell Death Dis. 9, 120.

Jansen, I.E., Savage, J.E., Watanabe, K., Bryois, J., Williams, D.M., Steinberg, S., Sealock, J., Karlsson, I.K., Hagg, S., Athanasiu, L., Voyle, N., Proitsi, P., Witoelar, A., Stringer, S., Aarsland, D., Almdahl, I.S., Andersen, F., Bergh, S., Bettella, F., Bjornsson, S., Braekhus, A., Brathen, G., de Leeuw, C., Desikan, R.S., Djurovic, S., Dumitrescu, L., Fladby, T., Hohman, T.J., Jonsson, P.V., Kiddle, S.J., Rongve, A., Saltvedt, I., Sando, S.B., Selbaek, G., Shoai, M., Skene, N.G., Snaedal, J., Stordal, E., Ulstein, I.D., Wang, Y., White, L.R., Hardy, J., Hjerling-Leffler, J., Sullivan, P.F., van der Flier, W.M., Dobson, R., Davis, L.K., Stefansson, H., Stefansson, K., Pedersen, N.L., Ripke, S., Andreassen, O.A., Posthuma, D., 2019. Genome-wide meta-analysis identifies new loci and functional pathways influencing Alzheimer's disease risk. Nat. Genet. 51, 404—413.

Kan, L., Israsena, N., Zhang, Z., Hu, M., Zhao, L.R., Jalali, A., Sahni, V., Kessler, J.A., 2004. Sox1 acts through multiple independent pathways to promote neurogenesis. Dev. Biol. 269, 580—594.

Klose, R.J., Bird, A.P., 2006. Genomic DNA methylation: the mark and its mediators. Trends Biochem. Sci. 31, 89—97.

Kumar, D., Sharma, A., Sharma, L., 2020. A comprehensive review of Alzheimer's association with related proteins: pathological role and therapeutic significance. Curr. Neuropharmacol.

Lahav-Ariel, L., Caspi, M., Nadar-Ponniah, P.T., Zelikson, N., Hofmann, I., Hanson, K.K., Franke, W.W., Sklan, E.H., Avraham, K.B., Rosin-Arbesfeld, R., 2019. Striatin is a novel modulator of cell adhesion. FASEB J. 33, 4729—4740.

Lambert, J.C., Ibrahim-Verbaas, C.A., Harold, D., Naj, A.C., Sims, R., Bellenguez, C., DeStafano, A.L., Bis, J.C., Beecham, G.W., Grenier-Boley, B., Russo, G., Thorton-Wells, T.A., Jones, N., Smith, A.V., Chouraki, V., Thomas, C., Ikram, M.A., Zelenika, D., Vardarajan, B.N., Kamatani, Y., Lin, C.F., Gerrish, A., Schmidt, H., Kunkle, B., Dunstan, M.L., Ruiz, A., Bihoreau, M.T., Choi, S.H., Reitz, C., Pasquier, F., Cruchaga, C., Craig, D., Amin, N., Berr, C., Lopez, O.L., De Jager, P.L., Deramecourt, V., Johnston, J.A., Evans, D., Lovestone, S., Letenneur, L., Morón, F.J., Rubinsztein, D.C., Eiriksdottir, G., Sleegers, K., Goate, A.M., Fiévet, N., Huentelman, M.W., Gill, M., Brown, K., Kamboh, M.I., Keller, L., Barberger-Gateau, P., McGuiness, B., Larson, E.B., Green, R., Myers, A.J., Dufouil, C., Todd, S., Wallon, D., Love, S., Rogaeva, E., Gallacher, J., St George-Hyslop, P., Clarimon, J., Lleo, A., Bayer, A., Tsuang, D.W., Yu, L., Tsolaki, M., Bossù, P., Spalletta, G., Proitsi, P., Collinge, J., Sorbi, S., Sanchez-Garcia, F., Fox, N.C., Hardy, J., Deniz Naranjo, M.C., Bosco, P., Clarke, R., Brayne, C., Galimberti, D., Mancuso, M., Matthews, F., Moebus, S., Mecocci, P., Del Zompo, M., Maier, W., Hampel, H., Pilotto, A., Bullido, M., Panza, F., Caffarra, P., Nacmias, B., Gilbert, J.R., Mayhaus, M., Lannefelt, L., Hakonarson, H., Pichler, S., Carrasquillo, M.M., Ingelsson, M., Beekly, D., Alvarez, V., Zou, F., Valladares, O., Younkin, S.G., Coto, E., Hamilton-Nelson, K.L., Gu, W., Razquin, C., Pastor, P., Mateo, I., Owen, M.J., Faber, K.M., Jonsson, P.V., Combarros, O., O'Donovan, M.C., Cantwell, L.B., Soininen, H., Blacker, D., Mead, S., Mosley Jr., T.H., Bennett, D.A., Harris, T.B., Fratiglioni, L., Holmes, C., de Bruijn, R.F., Passmore, P., Montine, T.J., Bettens, K., Rotter, J.I., Brice, A., Morgan, K., Foroud, T.M., Kukull, W.A., Hannequin, D., Powell, J.F., Nalls, M.A., Ritchie, K., Lunetta, K.L., Kauwe, J.S., Boerwinkle, E., Riemenschneider, M., Boada, M., Hiltuenen, M., Martin, E.R., Schmidt, R., Rujescu, D., Wang, L.S., Dartigues, J.F., Mayeux, R., Tzourio, C., Hofman, A., Nöthen, M.M., Graff, C., Psaty, B.M., Jones, L., Haines, J.L., Holmans, P.A., Lathrop, M., Pericak-Vance, M.A., Launer, L.J., Farrer, L.A., van Duijn, C.M., Van Broeckhoven, C., Moskvina, V., Seshadri, S., Williams, J., Schellenberg, G.D., Amouyel, P., 2013. Meta-analysis of 74,046 individuals identifies 11 new susceptibility loci for Alzheimer's disease. Nat. Genet. 45, 1452—1458.

Lawlor, D.A., Davey Smith, G., Kundu, D., Bruckdorfer, K.R., Ebrahim, S., 2004. Those confounded vitamins: what can we learn from the differences between observational versus randomised trial evidence? Lancet 363, 1724—1727.

Lawlor, D.A., Harbord, R.M., Sterne, J.A.C., Nic, T., George, D.S., 2008. Mendelian randomization: using genes as instruments for making causal inferences in epidemiology. Stat. Med. 27, 1133.

Lawlor, D.A., Smith, G.D., 2006. Cardiovascular risk and hormone replacement therapy. Curr. Opin. Obstet. Gynecol. 18, 658—665.

Lunnon, K., Smith, R., Hannon, E., De Jager, P.L., Srivastava, G., Volta, M., Troakes, C., Al-Sarraj, S., Burrage, J., Macdonald, R., Condliffe, D., Harries, L.W., Katsel, P., Haroutunian, V., Kaminsky, Z., Joachim, C., Powell, J., Lovestone, S., Bennett, D.A., Schalkwyk, L.C., Mill, J., 2014. Methylomic profiling implicates cortical deregulation of ANK1 in Alzheimer's disease. Nat. Neurosci. 17, 1164—1170.

Munari, F., Bortot, A., Assfalg, M., D'Onofrio, M., 2018. Alzheimer's disease-associated ubiquitin mutant Ubb(+1): properties of the carboxy-terminal domain and its influence on biomolecular interactions. Int. J. Biol. Macromol. 108, 24—31.

Ng, B., White, C.C., Klein, H.U., Sieberts, S.K., McCabe, C., Patrick, E., Xu, J., Yu, L., Gaiteri, C., Bennett, D.A., Mostafavi, S., De Jager, P.L., 2017. An xQTL map integrates the genetic architecture of the human brain's transcriptome and epigenome. Nat. Neurosci. 20, 1418—1426.

Nilsson, E., Jansson, P.A., Perfilyev, A., Volkov, P., Pedersen, M., Svensson, M.K., Poulsen, P., Ribel-Madsen, R., Pedersen, N.L., Almgren, P., Fadista, J., Ronn, T., Klarlund, P.B., Scheele, C., Vaag, A., Ling, C., 2014. Altered DNA methylation and differential expression of genes influencing metabolism and inflammation in adipose tissue from subjects with type 2 diabetes. Diabetes 63, 2962—2976.

Novotný, J., 2015. [Adenosine and its role in physiology]. Ceskoslovenska Fysiologie 64, 35—44.

Richardson, T.G., Haycock, P.C., Zheng, J., Timpson, N.J., Gaunt, T.R., Davey, S.G., Relton, C.L., Hemani, G., 2018. Systematic Mendelian randomization framework elucidates hundreds of CpG sites which may mediate the influence of genetic variants on disease. Hum. Mol. Genet. 27, 3293—3304.

Richardson, T.G., Zheng, J., Davey, S.G., Timpson, N.J., Gaunt, T.R., Relton, C.L., Hemani, G., 2017. Mendelian randomization analysis identifies CpG sites as putative mediators for genetic influences on cardiovascular disease risk. Am. J. Hum. Genet. 101, 590—602.

Sims, R., Hill, M., Williams, J., 2020. The multiplex model of the genetics of Alzheimer's disease. Nat. Neurosci. 23, 311—322.

Smith, R.G., Hannon, E., De Jager, P.L., Chibnik, L., Lott, S.J., Condliffe, D., Smith, A.R., Haroutunian, V., Troakes, C., Al-Sarraj, S., Bennett, D.A., Powell, J., Lovestone, S., Schalkwyk, L., Mill, J., Lunnon, K., 2018. Elevated DNA methylation across a 48-kb region spanning the HOXA gene cluster is associated with Alzheimer's disease neuropathology. Alzheimers Dement. 14, 1580—1588.

Teumer, A., 2018. Common methods for performing mendelian randomization. Front. Cardiovasc. Med. 5, 51.

Verbanck, M., Chen, C.Y., Neale, B., Do, R., 2018. Detection of widespread horizontal pleiotropy in causal relationships inferred from Mendelian randomization between complex traits and diseases. Nat. Genet. 50, 693—698.

Wahl, S., Drong, A., Lehne, B., Loh, M., Scott, W.R., Kunze, S., Tsai, P.C., Ried, J.S., Zhang, W., Yang, Y., Tan, S., Fiorito, G., Franke, L., Guarrera, S., Kasela, S., Kriebel, J., Richmond, R.C., Adamo, M., Afzal, U., Ala-Korpela, M., Albetti, B., Ammerpohl, O., Apperley, J.F., Beekman, M., Bertazzi, P.A., Black, S.L., Blancher, C., Bonder, M.J., Brosch, M., Carstensen-Kirberg, M., de Craen, A.J., de Lusignan, S., Dehghan, A., Elkalaawy, M., Fischer, K., Franco, O.H., Gaunt, T.R., Hampe, J., Hashemi, M., Isaacs, A., Jenkinson, A., Jha, S., Kato, N., Krogh, V., Laffan, M., Meisinger, C., Meitinger, T., Mok, Z.Y., Motta, V., Ng, H.K., Nikolakopoulou, Z., Nteliopoulos, G., Panico, S., Pervjakova, N., Prokisch, H., Rathmann, W., Roden, M., Rota, F., Rozario, M.A., Sandling, J.K., Schafmayer, C., Schramm, K., Siebert, R., Slagboom, P.E., Soininen, P., Stolk, L., Strauch, K., Tai, E.S., Tarantini, L., Thorand, B., Tigchelaar, E.F., Tumino, R., Uitterlinden, A.G., van Duijn, C., van Meurs, J.B., Vineis, P., Wickremasinghe, A.R., Wijmenga, C., Yang, T.P., Yuan, W., Zhernakova, A., Batterham, R.L., Smith, G.D., Deloukas, P., Heijmans, B.T., Herder, C., Hofman, A., Lindgren, C.M., Milani, L., van der Harst, P., Peters, A., Illig, T., Relton, C.L., Waldenberger, M., Jarvelin, M.R., Bollati, V., Soong, R., Spector, T.D., Scott, J., McCarthy, M.I., Elliott, P., Bell, J.T., Matullo, G., Gieger, C., Kooner, J.S., Grallert, H., Chambers, J.C., 2017. Epigenome-wide association study of body mass index, and the adverse outcomes of adiposity. Nature 541, 81—86.

Watson, C.T., Roussos, P., Garg, P., Ho, D.J., Azam, N., Katsel, P.L., Haroutunian, V., Sharp, A.J., 2016. Genome-wide DNA methylation profiling in the superior temporal gyrus reveals epigenetic signatures associated with Alzheimer's disease. Genome Med. 8, 5.

Weidner, C.I., Lin, Q., Koch, C.M., Eisele, L., Beier, F., Ziegler, P., Bauerschlag, D.O., Jockel, K.H., Erbel, R., Muhleisen, T.W., Zenke, M., Brummendorf, T.H., Wagner, W., 2014. Aging of blood can be tracked by DNA methylation changes at just three CpG sites. Genome Biol. 15, R24.

Yavorska, O.O., Burgess, S., 2017. MendelianRandomization: an R package for performing Mendelian randomization analyses using summarized data. Int. J. Epidemiol. 46, 1734—1739.

Yu, G., Wang, L.G., Han, Y., He, Q.Y., 2012. clusterProfiler: an R package for comparing biological themes among gene clusters. Omics 16, 284—287.

Yu, L., Chibnik, L.B., Srivastava, G.P., Pochet, N., Yang, J., Xu, J., Kozubek, J., Obholzer, N., Leurgans, S.E., Schneider, J.A., Meissner, A., De Jager, P.L., Bennett, D.A., 2015. Association of Brain DNA methylation in SORL1, ABCA7, HLA-DRB5, SLC24A4, and BIN1 with pathological diagnosis of Alzheimer disease. JAMA Neurol. 72, 15—24.

Zhou, Y., Zhou, B., Pache, L., Chang, M., Khodabakhshi, A.H., Tanaseichuk, O., Benner, C., Chanda, S.K., 2019. Metascape provides a biologist-oriented resource for the analysis of systems-level datasets. Nat. Commun. 10, 1523.

Zhu, Z., Lin, Y., Li, X., Driver, J.A., Liang, L., 2019. Shared genetic architecture between metabolic traits and Alzheimer's disease: a large-scale genome-wide cross-trait analysis. Hum. Genet. 138, 271—285.

Zhu, Z., Zhang, F., Hu, H., Bakshi, A., Robinson, M.R., Powell, J.E., Montgomery, G.W., Goddard, M.E., Wray, N.R., Visscher, P.M., Yang, J., 2016. Integration of summary data from GWAS and eQTL studies predicts complex trait gene targets. Nat. Genet. 48, 481—487.